

# 1 $\nu_\mu$ CC $\pi^0$ Selection

## 2 1.1 Signal Definition

3 The  $\nu_\mu$  CC  $\pi^0$  signal definition encompasses charged-current neutrino interac-  
4 tions occuring within the fiducial volume of the detector and containing

- 5 • exactly one primary muon
- 6 • exactly zero charged pions
- 7 • exactly one neutral pion
- 8 • any number of particles that are not muons or pions.

9 This signal definition applies to final state particles, or particles exiting the  
10 target nucleus post-final state interactions (FSI).

11 Additional requirements are placed on the signal definition to ensure tracking  
12 thresholds are met and selection purity and efficiency are optimized. These are  
13 referred to as phase space constraints and include:

- 14 •  $p_\mu > 226$  MeV/c
- 15 •  $p_{\pi^0} > 100$  MeV/c.

## 16 1.2 Selection Cuts

17 When selecting  $\nu_\mu$  CC  $\pi^0$  interactions, cuts are made on various reconstructed  
18 outputs to narrow the list of candidate interactions. First, the reconstructed  
19 interaction is required to occur within the ICARUS fiducial volume. The inter-  
20 action must then pass a topology cut, enforcing inclusion of exactly one primary  
21 muon, zero primary charged pions, and two primary photons as reported by the  
22 ML reconstruction chain's primary particle classification and particle identifica-  
23 tion algorithms. The particles within an interaction must also meet the phase  
24 space constraints of the signal definition, necessitating methods to estimate  
25 particle energy and momentum. These methods are discussed in Section 1.4.  
26 Finally, the interaction is required to be associated with an optical flash that is  
27 in-time with the NuMI beam gate, as determined by the Opt0Finder algorithm.  
28 When these criteria are met, the interaction is considered a candidate  $\nu_\mu$  CC  
29  $\pi^0$  interaction.

## 30 1.3 Selection Performance

31 Selection performance is assessed using the NuMI  $\nu$  + Cosmic MC sample and  
32 off-beam NuMI Run 2 data. The metrics that have been evaluated are efficiency  
33 - the fraction of true signal interactions are matched to selected interactions,  
34 and purity - the fraction of selected interactions are matched to true signal  
35 interactions. Figure 1 shows the selection efficiency for  $\nu_\mu$  CC  $\pi^0$  events before  
36 muon and neutral pion momentum thresholds are applied. The sharp drop-offs

at 226 MeV/c and 100 MeV/c for the muon and neutral pion distributions,  
 respectively, motivate the phase space constraints of the signal definition.



Figure 1: A missing figure.

Overall, the selection achieves an efficiency of 80% and a purity of 80%. Efficiency and purity for each selection cut are shown in Table 1. Signal inefficiencies are further characterized in the confusion matrix shown in Figure 2, while the backgrounds that lead to impurities are seen in Section 1.4.

Table 1: Purity and efficiency for  $\nu_\mu$  CC  $\pi^0$  Selection Cuts

Selection Cut	Purity [%]	Efficiency [%]
No Cut	xx	xx
Fiducial Volume	xx	xx
Final State Topology	xx	xx



Missing Figure

Figure 2: A missing figure.

## 1.4 Variables of Interest

In this section, the kinematic observables used in the single differential cross section measurement are discussed. Included are the momenta of the final state muon and neutral pion, as well as the angles these particles make with the NuMI beam. An additional variable, the invariant diphoton mass, is examined as it serves as a useful standard candle in the calibration of the electromagnetic shower energy scale. First, however, the methods used to estimate the energy (and momentum) of the reconstructed particles of interest is detailed.

### 1.4.1 Energy Reconstruction

To estimate the momentum of the reconstructed muon, a “best estimate” approach is taken. For muons contained within the active detector volume, momentum is calculated using the Continuous Slowing Down Approximation (CSDA) that relates a particle’s kinetic energy to its range in a material. For momentum estimation of exiting muons, the degree of multiple coulomb scattering (MCS) along the track is instead used. Figure 3 shows how each muon momentum estimate compares with true muon momentum in simulation.



Missing Figure

Figure 3: A missing figure.

59 Unlike muons, neutral pions do not directly ionize the detector medium. The  
60 neutral pion momentum must therefore be inferred from the electromagnetic  
61 showers instigated by the photons it decays to. Shower energy (and momentum)  
62 is estimated calorimetrically by summing charge depositions belonging to the  
63 shower and accounting for various detector effects:

$$E_{shower} = W_i \left[ \frac{MeV}{e^-} \right] \cdot C_{cal} \left[ \frac{e^-}{ADC} \right] \cdot C_{adj} \cdot \frac{1}{R} \cdot \sum_{dep} e^{\frac{t_{drift}}{\tau}} \cdot dep[ADC], \quad (1)$$

64 where

- 65  $W_i$  is the work function for argon
- 66  $C_{cal}$  converts charge units from ADC to electrons
- 67  $C_{adj}$  accounts for missing energy due to subthreshold charge and clustering
- 68 effects in reconstruction
- 69  $R$  is the recombination factor
- 70  $\tau$  is the electron lifetime
- 71  $dep$  is charge in units of ADC.

72 As the signal definition for this analysis does not require showers to be contained,  
73 an additional correction factor is needed to correct for missing energy in exiting  
74 showers. A study for deriving this factor is ongoing with results expected soon.

75 **1.4.2 Muon Observables**

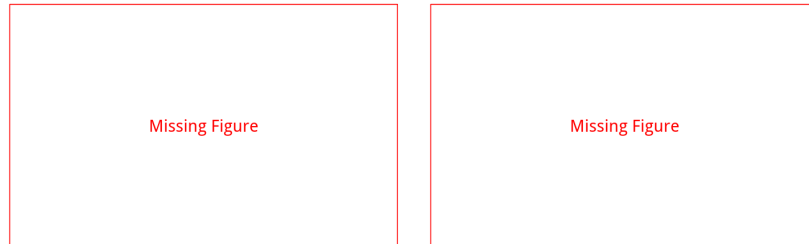


Figure 4: A missing figure.

76 **1.4.3 Photon Observables**

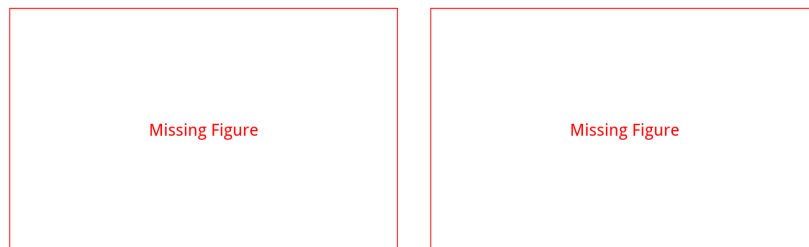


Figure 5: A missing figure.

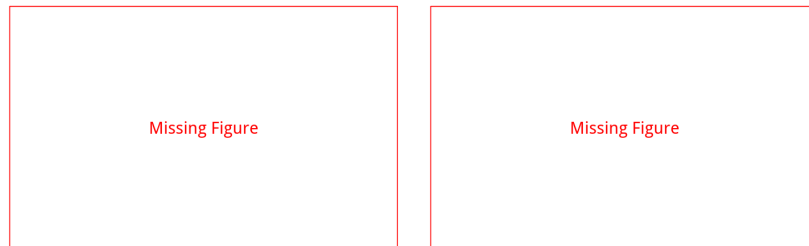


Figure 6: A missing figure.

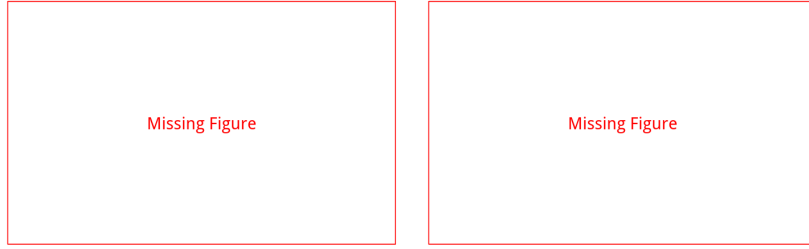


Figure 7: A missing figure.

<sup>77</sup> **1.4.4 Neutral Pion Observables**

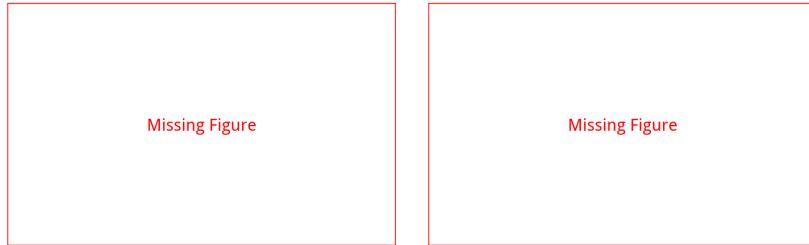


Figure 8: A missing figure.



Figure 9: A missing figure.